International Journal of Industrial Electronics, Control and Optimization © 2022 IECO
Vol. 5, No. 2, pp. 123-132, April (2022)

# An Enhanced Distributed State Feedback for Secondary Control in an Islanded Microgrid

Morteza Alizadeh[1], Hossein Askarian.A[2†], Alireza Bakhshai[3] , Naser Khodabakhshi-Javinani[4]

[1,2] Department of Electrical Engineering, Amirkabir University of Technology
[3] Department of Electrical and Computer Engineering, Queen's University Kingston, ON, Canada
[4] Electrical and Computer Engineering Department, Yadegar-e-Imam Khomeini (RAH) Shahre Rey Branch, Islamic Azad University, Tehran, Iran.

**ABSTRACT**

*This paper applies a new state feedback control to a distributed secondary voltage and frequency control in an islanded microgrid. The problem is focused on the output consensus of the multi-agent systems, which is converted to a first-order dynamic system. The inverter-based distributed generations play as agents in the proposed control strategy. It is assumed that the distributed generators communicate through a communication network modeled by a directed graph (digraph). The distributed output consensus is used to design the secondary controllers. Such innovative controllers synchronize distributed generators' output voltages and frequencies to their reference values by a novel state feedback approach. Compared to the existing consensus protocols, the proposed method provides a different innovative solution to the secondary voltage and frequency control of microgrids, which has a better response in case of communication failures. Finally, extensive and comparative simulations have been presented to verify the validity of the proposed control strategy and the system performance.*

**Article Info**

***Research Article***

***Keywords:***

Distributed cooperative control, Islanded microgrid, State feedback control, Secondary voltage control, Secondary frequency control

***Article History:***

**Received** 2021-12-26
**Accepted** 2022-02-20

## I. INTRODUCTION

Microgrids (MGs), consisting of distributed generators (DGs), loads, energy storages, power converters, LC filters, and output connectors, has recently been introduced and used to decrease the energy problems. Conventionally, MG can be operated in grid-connected, off-grid, or so-called islanded mode. MGs will change the traditional power generation structure and thus bring up new control challenges for the safe and efficient operation of the power system [1-5]. When islanded, voltage and frequency control of MGs become very important. In the well-known hierarchical control structure of MGs, secondary control restores voltage and frequency deviations caused by the primary control level to their reference values [6, 7]. Generally speaking, the secondary control uses a centralized structure that is required to send all the information of the DGs to a central control unit via a communication network system [8-11]. Information centralization provides reliability and security concerns. Also, centralized controllers have low-performance responses to plug-and-play and communication failures [9]. Moreover, the centralized methods do not satisfy accurate power-sharing [9].

In order to overcome the weaknesses mentioned above, several studies have suggested the so-called distributed secondary voltage and frequency control based on multi-agent systems [12-14]. Unlike a central controller, the distributed one works with a one-way communication network, and the agents only use their information and the information obtained from their just immediate neighbors. Therefore, the complex communication network of the centralized controllers is ignored. In particular, the upfront costs of communication infrastructure are decreased in distributed control approach. Moreover, in spite of the fact that centralized control has the

†**Corresponding Author**: askarian@aut.ac.ir
Tel: +98-2164543370, Fax: +98-2164543370, Electrical Engineering Department, Amirkabir University of Technology, Tehran, Iran

Copyright © 2022 Askarian et al. Published by University of Sistan and Baluchestan. This work is licensed under a Creative Commons Attribution-Noncommercial 4.0 International license. (https://creativecommons.org/licenses/by-nc/4.0/). Non-commercial uses of the work are permitted, provided the original work is properly cited

low plug-and-play capability, poor scalability, and weak response to communication failures, the distributed controller better handles the plugging out/in of any DGs and works more reliable in conditions of different communication failure. It is also worth noting that distributed control has persistent operation against time-varying communication graph topologies. In summary, all advantages of distributed controllers lead to efficient information sharing and allow the operator to make faster decisions.

As mentioned before, the secondary control's main aim is to restore the voltage and frequency of islanded MGs to their nominal references values. Also, a distributed approach is considered in the secondary control to share active power accurately when two or more DGs are working in parallel. Recently, researchers have shown an increased interest in distributed secondary voltage and frequency and active power-sharing control in AC microgrids [12-24]. Unlike frequency, a global variable in a microgrid, voltage is a local variable. Three different scenarios can be considered for voltage restoration through distributed secondary control in MGs, by (i) average voltage consensus in the whole MG [12, 13], (ii) accurate voltage consensus in the output of the voltage-controlled voltage source inverters (VSIs) [14, 15], or (iii) accurate voltage consensus in some specific busses in the MG [16]. Moreover, various distributed secondary control consider some limitations. For instance, in [17], the distributed secondary control (DSC) is utilized to implement a coordinated framework for multiple DGs grouped dynamically through smart switches in a microgrid. A DSC scheme is considered in [18] for a hybrid microgrid to control only the load voltage. Another DSC is provided by [19] to restore frequency and share active power in an AC microgrid with mobile emergency resources (MERs) during a specified time. DSC approach is also considered under sensor and actuator faults [20, 21], switching topologies [22], and variable time-delayed communications [23] or fixed-time delays [24].

Up to now, previous studies in the area of distributed secondary voltage and frequency control have examined initial cooperative consensus protocol. However, a novelty in the choice of consensus protocol has not been found in the literature. All the researches mentioned above have used conventional distributed control to restore voltage and frequency to their reference values and share active power accurately. However, in this paper, we enhanced the conventional DSC through an auxiliary part based on state information to improve the performance of the control protocol, such as accelerating the convergence speed and improving transient response. The proposed approach has a better performance than the conventional DSC approach in the presence of different power disturbances and communication failures.

In this paper, a new cooperative control based on state feedback control for a multi-agent system is considered to solve the secondary voltage and frequency control problem in an

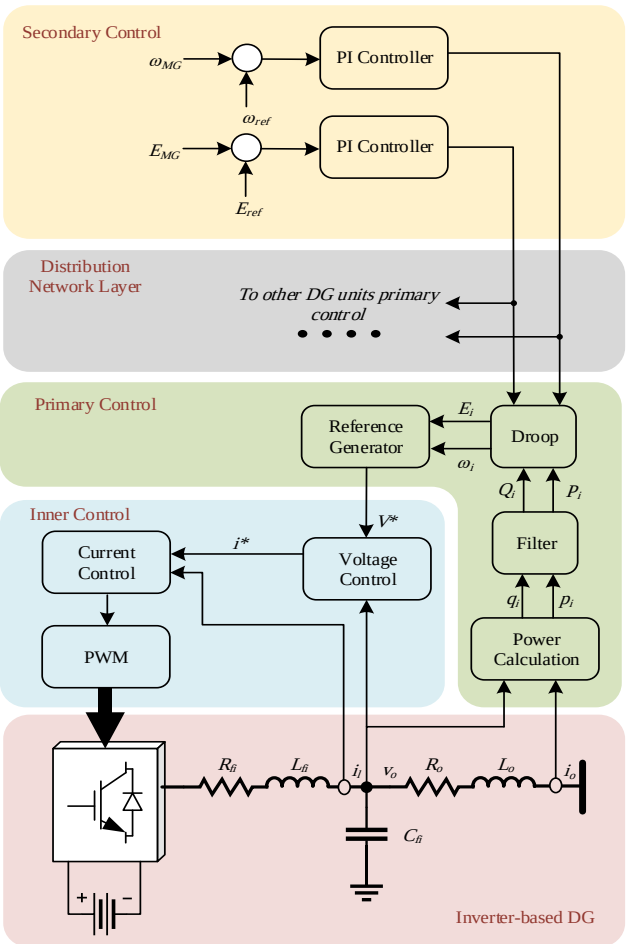



**Fig. 1.** Schematic diagram of an inverter-based DG with its three control levels

islanded MG. The problem is converted to a single integrator dynamic system to design a simple controller. It is considered that the multi-agent system is fully distributed, and all agents only use their information and information from their immediate neighbors. Simulations are performed to investigate all the implementation mentioned above concerns of distributed control. The proposed method is compared with the classical consensus protocol, and simulation results show that our method performs better, particularly in the presence of system and communication disturbances compared to the classical protocols.

The rest of this paper is organized as follows: Section II provides a brief review of the hierarchical structure of MG control. Section III presents a brief graph-theoretic preliminary and explains the problem statement. A novel output consensus with state feedback control is offered in Section IV. Section V and VI discuss problem formulation of distributed voltage and frequency control for an islanded MG, respectively. Section VII introduces the MG test system with four inverter-based DGs as a multi-agent system. Simulation studies and results analysis

are provided in Section VIII, and finally, the conclusions are drawn in Section IX.

## II. Hierarchical Structure of MG Control

In this section, the conventional hierarchical structure of MG control is reviewed. This control structure consists of four levels, including inner loop (zero), primary, secondary, and tertiary control levels responsible for processing, adjusting, monitoring, and optimizing system variables, respectively. Since the aim of this paper is to control secondary voltage and frequency in an islanded MG, the tertiary control level is not taken into consideration. For a detailed explanation, see [8, 25]. Fig. 1 shows an inverter-based DG schematic diagram with three control levels. The electrical network includes a dc power source, a three-leg dc-ac inverter, an LC filter, and an RL output connector. In the following, each control level of the hierarchical control structure is discussed.

### A. Inner Loop Control (Zero Level)

In this control level, the power is generated by using voltage-controlled voltage source inverters (VSIs), which are connected to an islanded MG, or current-controlled VSIs, which are connected to a grid-connected MG. As shown in Fig. 1, voltage-controlled VSIs consist of an inner current loop and an external voltage loop to stabilize the current and voltage and provide sufficient damping. While current-controlled VSIs are equipped with an inner current loop and a phase-locked loop to keep the synchronization with the grid. In the islanded mode of operation, a reference voltage is generated by the upper control layer as a primary control level.

### B. Primary Control

The droop control method is employed when two or more VSIs are connected in parallel to eliminate circulating currents and share active and reactive powers between converters. Generally speaking, the droop control method provides operating frequency and reference voltage magnitude for the voltage control loop according to the active and reactive power of inverter-based DG, respectively. For inductive lines, the droop control functions of *i-th* DG can be defined as follows [6, 8, 25]

$$\omega_i = \omega^* - P_i m_p \tag{1}$$

$$E_i = E^* - Q_i n_q \tag{2}$$

Where: $\omega^*$ and $E^*$ are frequency reference and voltage magnitude, $P_i$ and $Q_i$ are measured active and reactive powers of *i-th* DG, and. $m_p$ and $n_q$ are droop coefficients that are selected according to active and reactive power ratings. The primary control of the proposed VSI is shown in Fig. 1.

### C. Secondary Control Level

Voltage and frequency deviations caused by the primary control level can be compensated via the secondary control level. If the load or generation changes in MGs, secondary control guarantees the zero error of voltage and frequency fluctuations. In order to compensate voltage and frequency deviations, we should measure the voltage and frequency at the point of common coupling (PCC), $\omega_{MG,}$ and $E_{MG}$, and compare them with their references, $\omega_{ref}$, and $E_{ref}$. Then, the error values passed through the compensators are sent to all DG's primary control levels via communication links. The proportional-integral (PI) type controller shown in Fig. 1, as a common controller to restore voltage and frequency, can be obtained as follows [8]

$$\Delta\omega = k_{p\omega}(\omega_{ref} - \omega_{MG}) + k_{i\omega}\int(\omega_{ref} - \omega_{MG}) \tag{3}$$

$$\Delta E = k_{pE}(E_{ref} - E_{MG}) + k_{iE}\int(E_{ref} - E_{MG}) \tag{4}$$

Where: $k_{p\omega}$, $k_{i\omega}$, $k_{pE,}$ and $k_{iE}$ are PI controller parameters. Conventionally, this controller can be implemented as a centralized secondary controller. However, as mentioned before, low reliability, complex communication network, and weak performance are significant drawbacks of the secondary centralized control approach.

## III. Preliminary of Graph-Theoretic and Problem Statement

### A. Graph Theory

The communication network of the multi-agent system can be displayed by using a directed graph (digraph) $\mathcal{G}= (V, E, A)$ of order $n$ with the set of nodes $V=\{v_1, v_2, \ldots, v_n\}$, edges (arcs) $E \subseteq V \times V$, and *adjacency matrix* $A=\left[a_{ij}\right] \in \mathbb{R}^{n\times n}$. We assume the graph is simple, i.e., no self-loops and no multiple edges between two identical pairs of nodes. The node $v_k$ represents the $k_{th}$ agent, and the arc $(v_i, v_j)$ shows the information flows and means the agent $j$ is the neighbor of agent $i$. The number of its neighbor defines the *degree* of a node. Letting $d_i$ be the degree of node $v_i$, then the *degree matrix* of a graph $\mathcal{G}$, $D \in \mathbb{R}^{n\times n}$, is given by $D$, $diag(d)$, $d = \left[d_1, \ldots, d_n\right]^T$. Besides, we assume $a_{ij}$ is positive ($a_{ij} > 0$) if $(v_i, v_j) \in E$, *and* $a_{ij} = 0$ otherwise. The *Laplacian matrix*, $L$, associated with the graph $\mathcal{G}$, can be defined as $L_{ii} = \sum_{j\neq i} a_{ij}$ and $L_{ij} = -a_{ij}$, $j \neq i$ where $L\mathbf{1}_n = 0$. A sequence of successive edges in the form of $\{(v_i,v_k), (v_k,v_l), \ldots, (v_m,v_j)\}$ is considered as a direct path from node $i$ to node $j$. A compact form can represent the Laplacian matrix as $L = D - A$. A directed graph is said to have or contain a directed *spanning tree* if a root node exists that has a direct path from that node to every other node in the graph. [26].

### B. Problem Statement

We use a multi-agent with $n$ followers and one leader in this paper. Consider $n$ identical linear-space of the followers as:

$$\begin{aligned} \dot{x}_i(t) &= Ax_i(t) + Bu_i(t), \\ y_i(t) &= Cx_i(t), \qquad i = 1, 2, \ldots, n, \end{aligned} \tag{5}$$

With state vectors $x_i \in \mathbb{R}^n$, control input $u_i \in \mathbb{R}^p$, and output vector $y_i \in \mathbb{R}^q$. It is assumed that the matrix pairs $(A, B)$ and $(A, C)$ are controllable and observable,

respectively. Moreover, it is supposed that all followers have at least one neighbor. The leader, denoted as 0, generates the reference signal, which can be viewed as the following form:

$$\begin{aligned} \dot{x}_0(t) &= Mx_0(t), \\ y_0(t) &= Nx_0(t), \end{aligned} \tag{6}$$

Where: $x_0 \in \mathbb{R}^n$ and $y_0 \in \mathbb{R}^q$ are state and output leader, respectively. Also, it is assumed that the matrix pair $(M, N)$ is observable. Moreover, suppose that the leader receives no information from any follower.

*Assumption 1* For the followers in (5), there exist solution pairs $(T_i, U_i)$ for $i = 1, 2, \ldots, n$ as we have

$$\begin{aligned} T_i M &= A T_i + B U_i \\ CP_i &= N. \end{aligned} \tag{7}$$

Also, we define the output error for each follower as follows

$$e_i(t) = y_i(t) - y_0(t), \qquad i = 1, 2, \ldots, n \tag{8}$$

Here, in this paper, we have a control object of developing a distributed cooperative controller to solve the consensus problem in a multi-agent system which obtains the output error $e \to 0$ as $t \to \infty$ for any initial condition.

## IV. Output Consensus with State Feedback Control

In this section, the consensus problem of the multi-agent system is solved by designing state feedback in contrast with the classical consensus protocols. In order to reach output consensus, a distributed protocol for the system (5) and the leader (6) is given as in [27]

$$\begin{aligned} \dot{h}_i(t) &= Mh_i(t) + F[\sum_{j=1}^{n} a_{ij}(h_j(t) - h_i(t)) \\ &\quad + b_i(x_0(t) - h_i(t))], \\ u_i(t) &= K_1 x_i(t) + K_2 h_i(t), \qquad i = 1, 2, ..., n, \end{aligned} \tag{9}$$

Where: $h_i(t)$ is an auxiliary state of the controller $F \in \mathbb{R}^{p \times n}$, is called the coupling gain, and $K_1, K_2 \in \mathbb{R}^{p \times n}$ are the controller feedback gains to be determined. $a_{ij}$ is the $(i, j)$ - entry of the adjacency matrix associated with the $\mathcal{G}$ and $b_i$ is called the pinning gain.

*Theorem 1:* Suppose that assumption 1 holds. The consensus problem of a multi-agent system of followers in (5) and the leader in (6) can be solved by the control protocol in (9) if the following two conditions are satisfied:

(1) $F = \sigma P$, where $\sigma$ is a positive constant such that $\sigma\lambda_{\min} > 1$ where $\lambda_{\min}$ is the minimum eigenvalue of $L+b$ and the positive matrix $P$ is a solution of the following Ricatti equation

$$PM + M^T P - 2P^2 < 0. \tag{10}$$

(2) $K_1$ and $K_2$ can be determined such that $A + BK_1$ is Hurwitz, and $K_2 = U_i - K_1 T_i$ where $(T_i, U_i)$ is the solution of (7).

*Proof*: Let $x = col(x_1, x_2, \ldots, x_n)$ and $h = col(h_1, h_2, \ldots, h_n)$. Considering (5) and (8), the overall closed-loop network dynamics can be obtained in the following form

$$\begin{aligned} \dot{x}_i(t) &= (A + BK_1)x_i(t) + BK_2 h_i(t), \\ \dot{h}_i(t) &= Mh_i(t) + F[\sum_{j=1}^{n} a_{ij}(h_j(t) - h_i(t)) \\ &\quad + b_i(x_0(t) - h_i(t))]. \end{aligned} \tag{11}$$

The compact form of a closed-loop system can be written as

$$\begin{aligned} \dot{x}(t) &= (A + BK_1)x(t) + BK_2 h(t), \\ \dot{h}_i(t) &= (I_n \otimes M - (L+b) \otimes F)h(t) + ((L+b) \otimes F)\zeta_0(t), \end{aligned} \tag{12}$$

Where: $b = diag(b_1, b_2, \ldots, b_n)$ and $\zeta_0(t) = 1_n \otimes x_0(t)$.

By defining $\tilde{x}(t) = [x^T(t), h^T(t)]^T$, (12) can be rewritten as the following form

$$\dot{\tilde{x}}(t) = \tilde{A}\tilde{x}(t) + \tilde{B}\zeta_0(t), \tag{13}$$

Where: $A + BK$ is Hurwitz. Hence, the matrix $\tilde{A}$ is Hurwitz, if and only if $I_n \otimes M - (L+b) \otimes F$ is Hurwitz. Since $L+b$ is a symmetric matrix, we define an orthogonal matrix $U$ such that

$$U(L+b)U^T = Q = diag(\lambda_1, \lambda_2, \ldots, \lambda_n), \tag{14}$$

Where: $\lambda_i$, $i = 1, 2, \ldots, n$, is the eigenvalue of the $L+b$ and the matrix $U$ satisfies $UU^T = I_n$. Therefore, from (14) we can write:

$$\begin{aligned} & I_n \otimes M - (L+b) \otimes F \\ &= I_n \otimes M - (L+b) \otimes \tau P \\ &= (U^T \otimes I_n)(I_n \otimes M - Q \otimes \tau P)(U \otimes I_n) \\ &= (U^T \otimes I_n)diag(M - \lambda_1 \tau P, M - \lambda_2 \tau P, \ldots \\ &\quad , M - \lambda_n \tau P)(U \otimes I_n) \\ &\le (U^T \otimes I_n)diag(M - P, M - P, \ldots, M - P)(U \otimes I_n) \end{aligned} \tag{15}$$

Then, it concludes from (10) that:

$$PM + M^T P - 2P^2 = P(M-P) + (M-P)^T P < 0 \tag{16}$$

(16) together with (15) achieves $I_n \otimes M - (L+b) \otimes F$ which is Hurwitz. Therefore, it can be obtained that the matrix $\tilde{A}$ is Hurwitz, and the overall closed-loop system in (11) is asymptotically stable.

At the next step, we will prove that the output error $e_i(t)$ in (9) will converge to zero $t \to \infty$. Consider $\dot{\tilde{x}}_i(t) = \dot{x}_i - T_i \dot{x}_0(t)$, then we can write

$$\begin{aligned} \dot{\tilde{x}}_i(t) &= \dot{x}_i - T_i \dot{x}_0(t) \\ &= Ax_i(t) + B(K_1 x_i(t) + K_2 h_i(t)) - T_i(Mx_0(t)) \\ &= (A + BK_1)x_i(t) + BK_2 h_i(t) - T_i M x_0(t) \end{aligned} \tag{17}$$

From (8) and $K_2 = U_i - K_1 T_i$, (17) can be written in the form of (18)

$$\begin{aligned} \dot{\tilde{x}}_i(t) &= (A + BK_1)x_i(t) + (BU_i - BK_1 T_i)h_i(t) \\ &\quad - (AT_i + BU_i)x_0(t) \\ &= (A + BK_1)\tilde{x}_i(t) + BK_2(h_i(t) - x_0(t)) \end{aligned} \tag{18}$$

It is easy to see that if $A+BK_1$ is Hurwitz, then $\lim_{t\to\infty}\tilde{x}_i(t)=0$

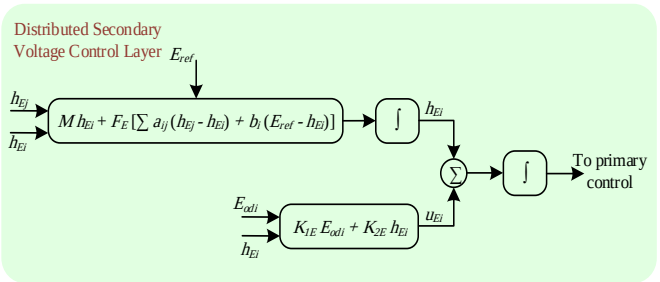



**Fig. 2**. The block diagram of the state feedback distributed secondary voltage control

. For the output error, we can derive (19)

$$\begin{aligned}\lim_{t\to\infty} e_i(t) &= \lim_{t\to\infty}(y_i(t)-y_0(t))\\ &= \lim_{t\to\infty}(Cx_i(t)-Nx_0(t))\\ &= \lim_{t\to\infty}(Cx_i(t)-CT_ix_0(t))\\ &= \lim_{t\to\infty}C(x_i(t)-T_ix_0(t))\\ &= \lim_{t\to\infty}C\tilde{x}_i(t)=0\end{aligned} \tag{19}$$

Which indicates the output error $e_i(t)\to 0$ as $t\to\infty$ for any initial condition. Therefore, the output consensus of the multi-agent followers (5) and the leader (6) is achieved by the protocol introduced in (8). This completes the proof.

## V. Distributed State Feedback for Secondary Voltage Control

In this section, an output consensus controller, based on the state feedback, is designed to solve the secondary voltage synchronization in an islanded MG. It is important to note that the dynamics of voltage and current controllers are overlooked in this study. This assumption is possible because their dynamics are much faster than the droop and power controllers. To do so, (2) can be rewritten in *dq* reference frame as

$$\begin{aligned}E_{odi} &= U_n - n_{qi}Q_i\\ E_{oqi} &= 0\end{aligned} \tag{20}$$

By differentiating the top equation in (20) we have (21).

$$\dot{U}_n = \dot{E}_{odi} + n_{qi}\dot{Q}_i \triangleq u_{Ei} \tag{21}$$

Where: $u_{Ei}$ is defined as an ancillary control. By employing (21) to a microgrid with *n* DGs the secondary voltage control of a microgrid can be changed to the consensus problem with first-order dynamics of the linear multi-agent system as follows:

$$\dot{E}_{odi} = u_{Ei}, \quad i=1,2,...,n \tag{22}$$

In order to solve the synchronization problem, it is assumed that DGs can communicate with each other over the prescribed graph $\mathcal{G}$ in section 3. All nodes of graph $\mathcal{G}$ have scalar single-integrator dynamics according to (22). It is worth noting that the protocol is fully distributed because each DG needs its own information and its neighbors under a low-band width communication network layer. In order to reach the output consensus of secondary voltage in an islanded MG, the following state feedback distributed consensus algorithm and the control inputs $u_{Ei}$ are considered, as described in (9) by (23):

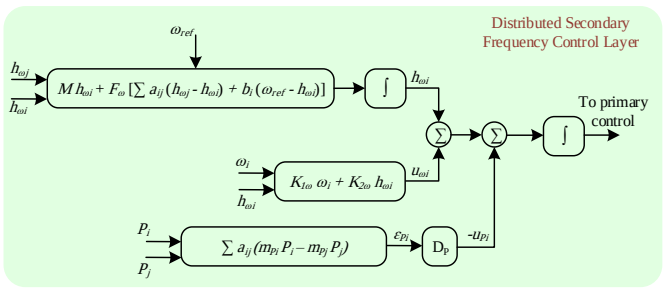



**Fig. 3.** The block diagram of the state feedback distributed secondary frequency control

$$\begin{aligned}\dot{h}_{Ei} &= M_E h_{Ei} + F_E\Big(\sum_{j=1}^{n} a_{ij}(h_{Ej}-h_{Ei}) + b_i(E_{ref}-h_{Ei})\Big)\\ u_{Ei} &= K_{1E}E_{odi} + K_{2E}h_{Ei}, \qquad i=1,2,...,n\end{aligned} \tag{23}$$

The block diagram of the proposed distributed secondary voltage control based on state feedback consensus algorithm is shown in Fig. 2.

## VI. Distributed State Feedback for Secondary Frequency Control

In this section, a distributed cooperative control based on state feedback control selects proper control inputs to synchronize the frequency of DGs, to the reference frequency, i.e. 50 Hz in this study. As the previous section, differentiating from (1) yields

$$\dot{\omega}_n = \dot{\omega}_i + m_{Pi}\dot{P} \triangleq u_{\omega i} \tag{24}$$

Where (24) determines the feedback linearization method providing the following dynamic linear multi-agent system.

$$\dot{\omega}_i = u_{\omega i}, \qquad i=1,2,...,n \tag{25}$$

We define state feedback distributed consensus algorithm the same as in (23), and the control inputs $u_{\omega i}$ for the frequency control are as follows

$$\begin{aligned}\dot{h}_{\omega i} &= M_\omega h_{\omega i} + F_\omega\Big(\sum_{j=1}^{n} a_{ij}(h_{\omega j}-h_{\omega i}) + b_i(\omega_{ref}-h_{\omega i})\Big)\\ u_{\omega i} &= K_{1\omega}\omega_i + K_{2\omega}h_{\omega i}, \qquad i=1,2,...,n\end{aligned} \tag{26}$$

As discussed in the previous section, the proposed control strategy provides the synchronization of all DG units' frequency to the reference value. According to (24), we can write (27).

$$\omega_i^* = \int(u_{\omega i} + m_{Pi}\dot{P})dt \tag{27}$$

Despite the fact that the term $n_{Qi}\dot{Q}_i$ in (21) is ineffective in voltage control in MGs, when frequency control is applied the active powers of DGs in an MG match (28).

$$\frac{P_j}{P_i} = \frac{m_{Pi}}{m_{Pj}} \tag{28}$$

In order to satisfy (28), another distributed cooperative consensus control for the term $m_{Pi}\dot{P}_i$ is supposed to ensure the accuracy of active power-sharing. Therefore, an auxiliary

control $u_{pi}$ is considered for the single-integrator and linear multi-agent system as follows:

$$m_{P_i}\dot{P}_i = u_{P_i}, \qquad i = 1, 2, ..., n \tag{29}$$

We consider a classical distributed cooperative consensus in order to synchronize the active powers of DGs with the same droop coefficients. By employing the local neighborhood tracking error of active powers $\varepsilon_{P_i}$ and the auxiliary control $u_{P_i}$ can be obtained as (30).

$$\begin{aligned} \varepsilon_{P_i} &= \sum_{j\in n} a_{ij}(m_{P_i}P_i - m_{P_j}P_j) \\ u_{P_i} &= -D_P\varepsilon_{P_i} \end{aligned} \tag{30}$$

In spite of (23) and (26) there is no second phrase in (30). Therefore, from Theorem 1 in [26], it can be realized that active powers with the same droop coefficients have to consensus with each other to ensure the active power sharing accuracy (i.e. $m_{Pk}$ $P_k \rightarrow m_{Pi}$ $P_i$).

Fig. 3 shows the complete block diagram of the proposed model based on a distributed secondary frequency control for both leader and follower DGs.

## VII. System Under Study

To evaluate the detailed analysis of the proposed state feedback distributed secondary voltage and frequency with the accurate active power-sharing, we have simulated a 380 V, 50 Hz islanded MG [14], as shown in Fig. 4, under the sequence of events in the MATLAB/SimPowerSystems software environment. The test system consists of four inverter-based DGs, three lines, and two loads. The lines and loads are modeled as series RL branches and constant real and reactive power, respectively. Table 1 gives the DGs, loads, and lines parameters of the MG test system. Also, the corresponding voltage and current controller parameters and droop coefficients are shown in Table 1. It is considered that DGs of MG are connected to each other through a directed graph communication network, as depicted in Fig. 5.

**TABLE 1.**
PARAMETERS OF THE MG TEST SYSTEM

| | | | | | |
|---|---|---|---|---|---|
| Line 1 & 3 | $R_{L1,3}$ | 0.23 Ω | Load 1 | $P_{load1}$ | 12 kW |
| | $L_{L1,3}$ | 0.318 mH | | $Q_{load1}$ | 12 kVAr |
| Line 2 | $R_{L2}$ | 0.35 Ω | Load 3 | $P_{load3}$ | 15.3 kW |
| | $L_{L2}$ | 1.847 mH | | $Q_{load3}$ | 7.6 kVAr |
| DG 1 & 2 | $m_P$ | $9.4 \times 10^{-5}$ | DG 3 & 4 | $m_P$ | $12.5 \times 10^{-5}$ |
| | $n_Q$ | $1.3 \times 10^{-3}$ | | $n_Q$ | $1.5 \times 10^{-3}$ |
| | $L_{f1}$, | 0.35 mH | | $L_{f3}$, $L_{f4}$ | 0.35 mH |
| | $R_{f1}$, | 0.03 Ω | | $R_{f3}$, $R_{f4}$ | 0.03 Ω |
| | $C_f$ | 50 μF | | $C_f$ | 50 μF |
| | $K_{PV}$ | 0.1 | | $K_{PV}$ | 0.05 |
| | $K_{IV}$ | 420 | | $K_{IV}$ | 390 |
| | $K_{PC}$ | 15 | | $K_{PC}$ | 10.5 |
| | $K_{IC}$ | 20000 | | $K_{IC}$ | 16000 |

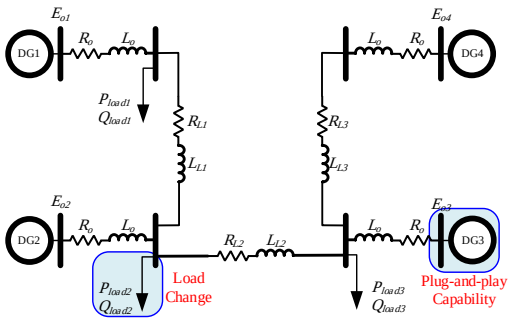



**Fig. 4.** The MG test system under study

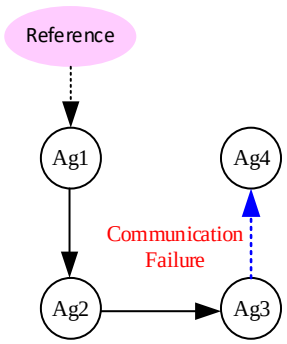



**Fig. 5.** Graph topology of the MG test system

## VIII. Discussion on Simulation Results

From (22) and (25), for the single-integrator dynamics, $A = 0, B = 1$ and as the leader dynamic is scalar in both voltage and frequency control, then it is concluded that in (6) that we have, $M = 0, N = 1$. According to the directed graph topology shown in Fig. 5, the matrix $L+b$ can be determined as follows:

$$L + b = \begin{bmatrix} 2 & 0 & 1 & 1 \\ 0 & 1 & -1 & 0 \\ 0 & 0 & 1 & -1 \\ 0 & 0 & 0 & 0 \end{bmatrix}$$

The minimum positive eigenvalue of the proposed matrix $\lambda_{\min} = 1$. Therefore, the first condition in Theorem 1 is satisfied by choosing $\sigma > 1$. Therefore, under condition (1) of *Theorem 1*, the Ricatti equation in (10) satisfies for any value of $P$, and from condition (2), it is deduced that for $K_1$, and $K_2$ we must have $K_1 < 0, and\ K_2 = -K_1$. Simulation results consist of three parts. At the first step, the controller performance is discussed, and, in another step, we investigate the controller gains impact on the speed convergence. Finally, we compare the proposed consensus protocol with the classic one presented in [14].

### A. Controller Performance

For the simulations of this part, we choose $K_{1E} = -60$, $K_{1\omega} = -30$, $F_E = 90$, $F_\omega = 50$ and $D_P = 70$, in order to have acceptable performance for the proposed controllers. Figs. 6 (a),

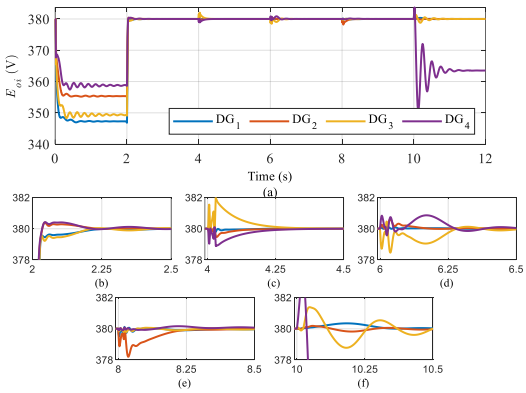



**Fig. 6.** DG output voltages with the proposed controller (a) Overall trajectory (b)- (f) Magnified trajectories

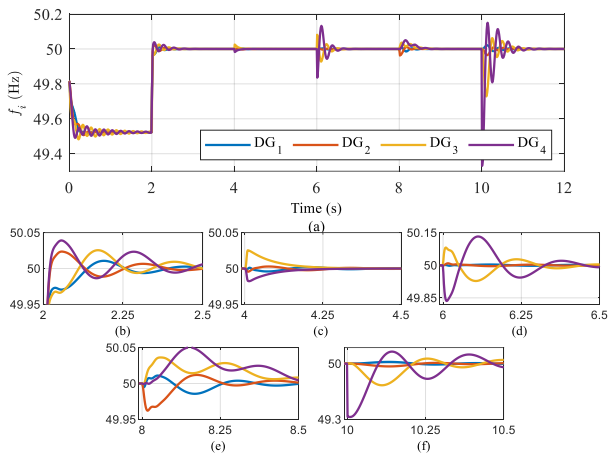



**Fig. 7.** DG frequencies with the proposed controller (a) Overall trajectory (b)- (f) Magnified trajectories

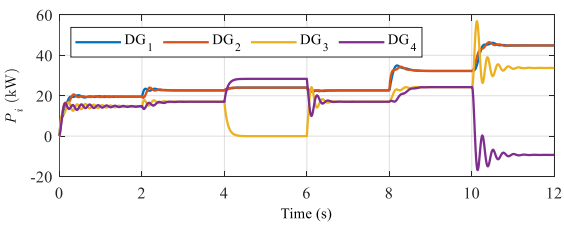



**Fig. 8.** DG active powers with the proposed controller

(b), and (c) show the output voltage, frequency, and active power of DGs, respectively, while distributed secondary voltage and frequency are activated. At $t$ = 0 s, only the primary control as discussed in section II is applied, and the secondary control is intentionally deactivated. As Figs. 6 (a) and (b) show, the DGs output voltage and the MG frequency stray from the reference values because of DGs droop controllers. In order to restore the output voltage of DGs and MG frequency, the state feedback distributed cooperative controls for secondary voltage and frequency control, as explained in sections V and VI, is applied at $t$ = 2 s, under the communication network shown in Fig. 5. It is shown that by applying the proposed distributed control, both voltage and frequency are rapidly restored to their reference values for all DGs. In the following, at $t$ = 4 s, for examining the plug-and-play capability, DG3 is plugged out from the MG and, at $t$ = 6, is reconnected to the MG. As shown in the zoomed Figs. 6 (c), (d) and 5 (c), and (d), both voltage and frequency have some acceptable fluctuations and restore to their reference values in finite-time (less than 1 sec). After that, at $t$ = 8 s, the *load2* with $P$ = 12 kW and $Q$ = 12 kVAr is applied to the MG. Again, Fig 6 and 7 (e) show that the deviations of both voltage and frequency are damped in finite-time (less than 1 sec). Finally, at $t$ = 8 s, the communication link between DG3 and DG4, as shown in Fig. 5 in the dashed line, is failed. The simulation results as depicted in zoomed pictures Fig. 6 and 7 (f) show that the proposed consensus protocol synchronizes voltage and frequency of three DGs to the reference values in finite-time, and the DG4 voltage is reduced to the 364.3 V because it separates from the graph topology. Since the frequency is a global parameter the DG4 frequency holds at 50 Hz. Also, Fig. 8 displays the active power of four DGs with the proposed consensus controller. Simulation results show that accurate active power-sharing is achieved by the proposed controller.

### *B. Controller Gains Effect*

To investigate the effect of controller gains on the dynamic response of the outputs, we consider three different sets of values for $K_{1E}$, $K_{2E}$, $K_{1\omega}$ and $K_{2\omega}$. The effect of different controller gains on the dynamic response of the output error as in (8) for voltage and frequency of DG2, i.e., $e_{E3}$ and $e_{\omega 3}$, is depicted in Fig. 9 (a) and (b), respectively. According to the simulation results, there is a clear trend of increase in the convergence speed with the growth of control gains in output error of voltage, as shown in Fig. 9 (a). Also, from Fig. 9 (b), it is clear that the frequency output error for the $K_{1\omega} = -10$ (the blue chart) has the slowest convergence compared with the one with $K_{1\omega} = -120$ (the red chart). From Figs. 9, it is clear that for the higher values of the controller gains, there is no significant development in speed convergence and dynamic response.

### *C. Controller Performance Compared with [14]*

In this subsection, the proposed controller is compared with the classical consensus protocol proposed in [14]. As previously noticed in the introduction, the classical consensus protocol performance is not evaluated in existing studies. Since the proposed protocol is applied in the homogenous single-integrator systems as shown in (22), (25), and (29), which is the same as in [14], we compare the proposed controller with the one presented in [14]. In order to study the performance of both controllers, we select the output voltage and the frequency of DG3, as depicted in Fig. 10 and Fig. 11, respectively. The gain controllers are chosen as both controllers have almost the same response at $t$ = *2*, i.e., the time that secondary distributed control is applied. Simulation results in Fig. 10 show that the proposed consensus protocol rapidly reaches consensus and, especially,

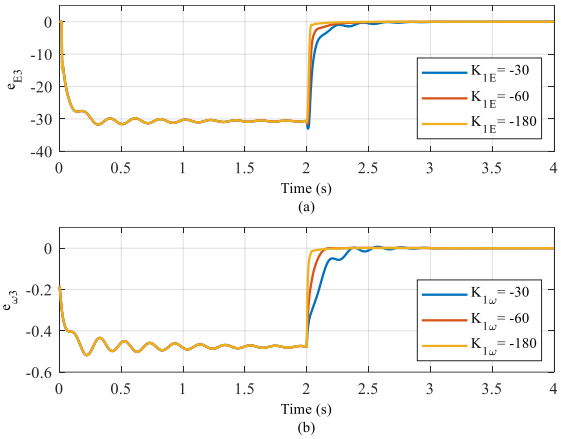



**Fig. 9.** Output error of DG3 for (a) Voltage (b) Frequency

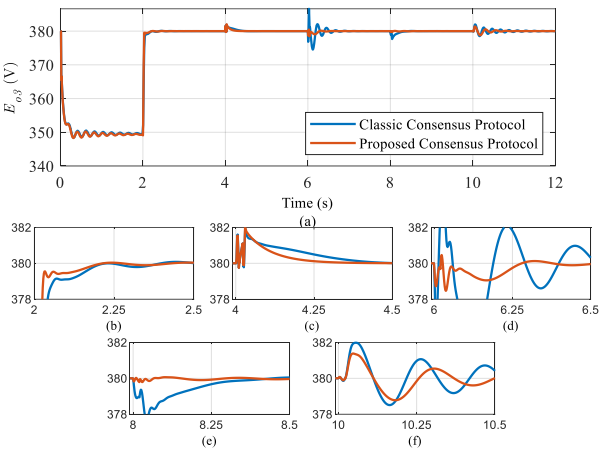



**Fig. 10**. Comparison between the proposed and the classical

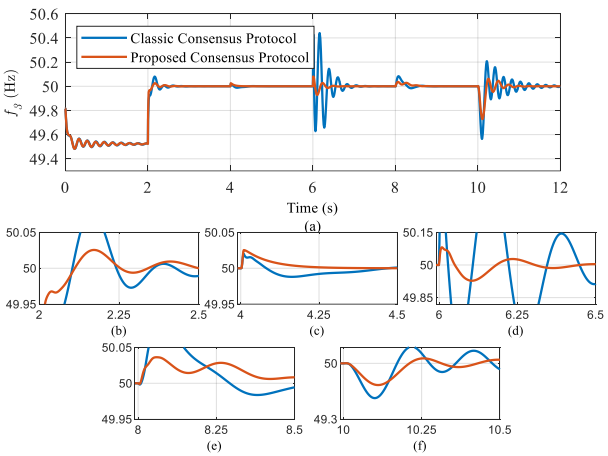



**Fig. 11.** Comparison between the proposed and the classical consensus protocols in [14] for the frequency of DG3 (a) Overall trajectory (b)- (f) Magnified trajectories

in plug-and-play and load changes has more robust performance than the classical protocol presented in [14].

Fig. 11 shows the frequency of DG3 with the proposed consensus protocol compared with the classical protocol studied in [14]. As seen from Fig. 9 it is clear that our protocol has a better response in comparison to the classical consensus protocol. Again, in particular, in plug-and-play capability, load changes, and communication failure, the proposed protocol has a more appropriate response.

## IX. Conclusions

New state feedback distributed voltage and frequency of an islanded MG is proposed in this paper. The MG is considered with DGs that can communicate through a communication graph topology. The secondary voltage and frequency problem is converted to a simple single integrator consensus problem with a scalar controller gain by feedback linearization. Two state feedback distributed consensus algorithms for output voltage frequency and one classical distributed cooperative consensus protocols in [14] for the output voltage of DG3 (a) Overall trajectory (b)- (f) Magnified trajectories approach for output real power demonstrate active power-sharing among DGs. Despite a centralized control structure, the proposed controller only works with the information of some neighbors' DGs. The designed controller is very simple and has not been proposed or investigated for secondary voltage and frequency control of MGs before. A number of simulation studies were carried out in MATLAB/SimPowerSystems to show the effectiveness of the controller. Simulation results show that the prescribed state feedback control strategy has a significant performance in restoring voltage and frequency to their reference values and has the ability to change the convergence speed directly by adjusting the controller gains.

## References

[1] R. H. Lasseter, "Microgrids," in *2002 IEEE Power Engineering Society Winter Meeting. Conference Proceedings (Cat. No. 02CH37309)*, 2002, vol. 1, pp. 305-308: IEEE.

[2] R. H. Lasseter, "Smart distribution: Coupled microgrids," *Proceedings of the IEEE*, vol. 99, no. 6, pp. 1074-1082, 2011.

[3] "Microgrids and active distribution networks," *The institution of Engineering Technology*, 2009.

[4] F. Katiraei, R. Iravani, N. Hatziargyriou, and A. Dimeas, "Microgrids management," *IEEE power energy magazine*, vol. 6, no. 3, pp. 54-65, 2008.

[5] E. Hossain, E. Kabalci, R. Bayindir, R. Perez, and Management, "Microgrid testbeds around the world: State of art," *Energy Conversion*, vol. 86, pp. 132-153, 2014.

[6] A. Bidram and A. Davoudi, "Hierarchical structure of microgrids control system," *IEEE Transactions on Smart Grid*, vol. 3, no. 4, pp. 1963-1976, 2012.

[7] J. M. Guerrero, M. Chandorkar, T.-L. Lee, and P. C. Loh, "Advanced control architectures for intelligent microgrids—Part I: Decentralized and hierarchical control," *IEEE Transactions on Industrial Electronics*, vol. 60, no. 4, pp. 1254-1262, 2012.

[8] J. M. Guerrero, J. C. Vasquez, J. Matas, L. G. De Vicuña, and M. Castilla, "Hierarchical control of droop-controlled AC and DC microgrids—A general approach toward standardization,"

*IEEE Transactions on industrial electronics*, vol. 58, no. 1, pp. 158-172, 2010.

[9] T. Morstyn, B. Hredzak, and V. G. Agelidis, "Control strategies for microgrids with distributed energy storage systems: An overview," *IEEE Transactions on Smart Grid*, vol. 9, no. 4, pp. 3652-3666, 2016.

[10] A. Mehrizi-Sani and R. Iravani, "Potential-function based control of a microgrid in islanded and grid-connected modes," *IEEE Transactions on Power Systems*, vol. 25, no. 4, pp. 1883-1891, 2010.

[11] C. Yang *et al.*, "Dynamic event-triggered robust secondary frequency control for islanded AC microgrid," *Applied energy*, vol. 242, pp. 821-836, 2019.

[12] Q. Shafiee, J. M. Guerrero, and J. C. Vasquez, "Distributed secondary control for islanded microgrids—A novel approach," *IEEE Transactions on power electronics*, vol. 29, no. 2, pp. 1018-1031, 2013.

[13] J. W. Simpson-Porco, Q. Shafiee, F. Dörfler, J. C. Vasquez, J. M. Guerrero, and F. Bullo, "Secondary frequency and voltage control of islanded microgrids via distributed averaging," *IEEE Transactions on Industrial Electronics*, vol. 62, no. 11, pp. 7025-7038, 2015.

[14] A. Bidram, A. Davoudi, F. L. Lewis, and Z. Qu, "Secondary control of microgrids based on distributed cooperative control of multi-agent systems," *IET Generation, Transmission Distribution*, vol. 7, no. 8, pp. 822-831, 2013.

[15] N. M. Dehkordi, N. Sadati, and M. Hamzeh, "Fully distributed cooperative secondary frequency and voltage control of islanded microgrids," *IEEE Transactions on Energy Conversion*, vol. 32, no. 2, pp. 675-685, 2016.

[16] G. Lou, W. Gu, W. Sheng, X. Song, and F. Gao, "Distributed model predictive secondary voltage control of islanded microgrids with feedback linearization," *IEEE Access*, vol. 6, pp. 50169-50178, 2018.

[17] Y. Du, X. Lu, J. Wang, and S. Lukic, "Distributed secondary control strategy for microgrid operation with dynamic boundaries," *IEEE Transactions on Smart Grid*, vol. 10, no. 5, pp. 5269-5282, 2018.

[18] Y. Jafarian, A. Karimi, and H. Bevrani, "Secondary voltage control in a hybrid microgrid," *International Journal of Industrial Electronics Control and Optimization*, vol. 2, no. 3, pp. 221-232, 2019.

[19] Q. Zhou, M. Shahidehpour, M. Yan, X. Wu, A. Alabdulwahab, and A. Abusorrah, "Distributed secondary control for islanded microgrids with mobile emergency resources," *IEEE Transactions on Power Systems*, vol. 35, no. 2, pp. 1389-1399, 2019.

[20] A. Afshari, M. Karrari, H. R. Baghaee, and G. B. Gharehpetian, "Distributed fault-tolerant voltage/frequency synchronization in autonomous AC microgrids," *IEEE Transactions on Power Systems*, vol. 35, no. 5, pp. 3774-3789, 2020.

[21] B. N. Alhasnawi, B. H. Jasim, and B. E. Sedhom, "Distributed secondary consensus fault tolerant control method for voltage and frequency restoration and power sharing control in multi-agent microgrid," *International Journal of Electrical Power & Energy Systems*, vol. 133, p. 107251, 2021.

[22] M. Raeispour, H. Atrianfar, H. R. Baghaee, and G. B. Gharehpetian, "Distributed LMI-based control of heterogeneous microgrids considering fixed time-delays and switching topologies," *IET Renewable Power Generation*, vol. 14, no. 12, pp. 2068-2078, 2020.

[23] Y. Du, H. Tu, H. Yu, and S. Lukic, "Accurate consensus-based distributed averaging with variable time delay in support of distributed secondary control algorithms," *IEEE Transactions on Smart Grid*, vol. 11, no. 4, pp. 2918-2928, 2020.

[24] S. Ullah, L. Khan, I. Sami, and N. Ullah, "Consensus-based delay-tolerant distributed secondary control strategy for droop controlled AC microgrids," *IEEE Access*, vol. 9, pp. 6033-6049, 2021.

[25] O. Palizban and K. Kauhaniemi, "Hierarchical control structure in microgrids with distributed generation: Island and grid-connected mode," *Renewable Sustainable Energy Reviews*, vol. 44, pp. 797-813, 2015.

[26] F. L. Lewis, H. Zhang, K. Hengster-Movric, and A. Das, *Cooperative control of multi-agent systems: optimal and adaptive design approaches*. Springer Science & Business Media, 2013.

[27] T. Han, Z.-H. Guan, B. Xiao, J. Wu, and X. Chen, "Distributed output consensus of heterogeneous multi-agent systems via an output regulation approach," *Neurocomputing*, 2019.



**Morteza Alizadeh** received the B.S and M.S degrees in electrical engineering from the Islamic Azad University and the University of Birjand, Birjand, Iran, respectively. Currently, he is working toward a Ph.D. degree in electrical engineering with the Amirkabir University of Technology, Tehran, Iran. His research interests include microgrid, distributed control systems in microgrids, power system control, and power system.



**H. Askarian Abyaneh** (SM'09) was born in Abyaneh, Iran. He received the Ph.D. degree in electrical power system engineering from the University of Manchester Institute of Science and Technology, Manchester, U.K., in 1988. Currently, he is a Professor with the Department of Electrical Engineering, Amirkabir University of Technology (AUT), Tehran, Iran. His research interests are relay protection, power quality, restructuring, and deregulation in power systems.



**Alireza Bakhshai** (Fellow, IEEE) received the B.Sc. and M.Sc. degrees from the Isfahan University of Technology, Isfahan, Iran, in 1984 and 1986, respectively, and the Ph.D. degree from Concordia University, Montreal, QC, Canada, in 1997, all in electrical engineering. He is currently a Faculty Member with the Department of Electrical and Computer Engineering, Queen's University and a Licensed Professional Engineer (P. Eng.) in Ontario. From 1986 to 1993 and from 1998 to 2004, he was a Faculty Member with the

Department of Electrical and Computer Engineering, Isfahan University of Technology. His research interests include high power electronics, distributed energy generation and conversion, microgrid and smart grid systems, and advanced control theories applied to power electronics converters.



**N. Khodabakhshi-Javinani** received a Ph.D. degree in Electrical Engineering from Amirkabir University of Technology (AUT). He is currently an Assistant Professor with the Electrical and Computer Engineering Department, Yadegar-e-Imam Khomeini (RAH) Shahre Rey Branch, Islamic Azad University, Tehran, Iran, and a Senior Research Associate with the Power System Protection, Amirkabir University of Technology, Tehran, Iran. Dr. Khodabakhshi-Javinani has a scientific cooperation with Prof. M.Abedi and Prof. H.Askarian A. His current research interests include Power System Protection, Monitoring, Operation, Control, and Signal Processing.